Structure of Waterborne Organic Composite Coatings

Y. Chevalier,*,† M. Hidalgo,†,‡,# J.-Y. Cavaillé,‡,§ and B. Cabane⊥

Laboratoire des Matériaux Organiques à Propriétés Spécifiques, LMOPS-CNRS, BP 24, 69390 Vernaison, France; Groupe d'Études de Métallurgie Physique et Physique des Matériaux, GEMPPM-INSA, av. A. Einstein, 69621 Villeurbanne Cedex, France; Centre de Recherches sur les Macromolécules Végétales, CERMAV-CNRS, BP 53, 38041 Grenoble Cedex 09, France; and Physique et Mécanique des Milieux Hétérogènes, PMMH, ESPCI, 10 rue Vauquelin, 75231 Paris Cedex 05, France

Received April 12, 1999; Revised Manuscript Received August 3, 1999

ABSTRACT: The mechanical properties and structure of composite films made of high-T_g polystyrene (PS) nodules dispersed in a low-T_g poly(butyl acrylate) (PBuA) matrix were studied by means of dynamic mechanical spectrometry and small-angle neutron scattering. At temperatures between the T_g of PS and PBuA, the mechanical properties depend drastically on the spatial distribution of the glassy PS domains. For films cast from mixtures of PS and PBuA latexes, an aggregation of PS particles into dense clusters dispersed in the PBuA matrix was observed. As a consequence, a large density of contacts between PS particles in the dry films ensured a strong mechanical reinforcement above a percolation threshold of 30% PS volume fraction. Extensive coalescence of PS particles occurred at their contacts upon annealing the films above the T_g of PS, leading to further mechanical reinforcement. For films cast from core−shell particles, the aggregation phenomenon was prevented, depending on the coverage of the PS core by the PBuA shell. An efficient core encapsulation in the core−shell morphology led to poor contact between PS cores, the elastic moduli were then close to that of the PBuA matrix, and the PS coalescence upon annealing was prevented.

Introduction

Waterborne organic coatings are gaining importance because of the use of water as a "solvent" instead of volatile organic compounds. Water resistance of the coatings imposes the utilization of water-insoluble organic polymers, which are used as their colloidal dispersions in water.[1,2] The formation of a dry film from an aqueous colloidal suspension of polymer particles takes place in different stages during water evaporation and in the dry state.[3−7] Thus, particles approach each other, stick, and finally get deformed from spheres to polyhedra as water evaporates.[8,9] The last stage of film formation known as the film maturation is the coalescence of the particles where macromolecules belonging to different particles mix by interdiffusion.[10−13] When the interdiffusion depth exceeds the radius of gyration of a macromolecule, the memory of the initial dispersion of particles is lost, and an homogeneous film with full tensile strength results.[11] Since the last interdiffusion stage requires the macromolecular mobility of the rubbery state of polymers, the film formation is allowed above the "minimum film formation temperature" (MFFT), close to the glass transition temperature (T_g) of the polymer. Dry films of such polymers have poor mechanical properties: elastic moduli and tensile strength are low, and large plastic deformations are attained at low stress levels. The mechanical properties can be improved by the addition of solid particles (fillers), either inorganic or organic (high-T_g polymer particles).[14−20] The moduli of the composite films can reach values that are close to that of the solid at high volume fractions of fillers, when a percolating network of these particles is formed.[18−20] Practical applications are the mechanical reinforcement of paints and adhesives by inorganic pigments,[1] and quite a large amount of work has been devoted to study the reinforcement of rubber by carbon blacks.[21,22] In particular, Payne recognized early the large contribution of the structure of the carbon black dispersion to the mechanical properties of rubber vulcanisates.[21]

In the case where the solid particles are made of a high-T_g polymer, the coalescence of the high-T_g polymer can be obtained by heating the films above its glass transition temperature, leading to a further structural transformation of the dry films. Thus, the weak "bonds" between solid particles at their points of contact are strengthened by polymer interdiffusion, resulting in a further increase of elastic modulus.[18,23] The mechanical properties depend on various parameters, the most important ones being the volume fraction of the high-T_g polymer particles, their size, and surface chemistry.[18,20,23−25] The structure of the high-T_g polymer particles dispersion in the dry film is a key parameter.[20] In particular, the building up of a continuous percolating network of solid particles requires efficient mechanical couplings between the solid particles.

Thus, systematic studies of the structure of composite films made of solid particles dispersed into a low-T_g polymer matrix have been carried out, looking for relationships between mechanical properties and film structure. In the present work, the mechanical properties and the structure of films made of glassy polystyrene (PS) particles in a soft poly(butyl acrylate) (PBuA) matrix were studied. The structure was studied by means of dynamic mechanical analysis (DMA) and small-angle neutron scattering (SANS), these two complementary methods providing structural information on very different scales. For heterogeneous materials composed of domains containing materials of very different

† LMOPS-CNRS.
‡ GEMPPM-INSA.
§ CERMAV-CNRS.
⊥ PMMH.
* Corresponding author.
# Current address: Elf-Atochem, 95 rue Danton, 92300 Levallois-Perret, France.

10.1021/ma990561e CCC: $18.00
Published on Web 10/27/1999

Table 1. Polymerization Recipe for the PS Latex Seeds and the Composite Latexes A and B (All Values in grams)

ingredient	PS seed	PS/PBuA (latex A)	PS/PBuA-*co*-MAA (latex B)
deionized water	1350	670	670
$NaHCO_3$	1	0.75	0.75
$K_2S_2O_8$	1	0.75	0.75
DDAPS emulsifier	4.5		
styrene	150		
PS seed		300	300
butyl acrylate (BuA)		45	41
methacrylic acid (MAA)			4

mechanical properties (elastic for PS and mainly viscous for PBuA), DMA[18] is sensitive to the large-scale structure (topological arrangement), whereas SANS[26,27] is a local method for structural investigations in the 1−100 nm range.

Materials and Methods

Materials. Styrene (S) from Prolabo, butyl acrylate (BuA), and methacrylic acid (MAA) from Merck were distilled under reduced pressure. The initiator potassium persulfate ($K_2S_2O_8$), $NaHCO_3$ from Merck, and the emulsifying agents, dodecyldimethylammoniopropanesulfonate from Fluka and sodium dodecyl sulfate (SDS) from Aldrich, were analytical grade products and used as received.

The polymerizations were carried out in a 1.5 L glass reactor, equipped with an anchor-type glass stirrer, a set of baffles to promote good mixing, a nitrogen inlet, and a reflux condensator. Stirring speed was 250 rpm.

Homogeneous Latexes. The PS and PBuA particles were obtained by batch emulsion polymerization at full conversion of styrene or butyl acrylate. Small PS particles with a narrow size distribution were prepared in the presence of the zwitterionic emulsifier dodecyldimethylammoniopropanesulfonate (DDAPS, $C_{12}H_{25}{}^{+}N(CH_3)_2-(CH_2)_3-SO_3{}^{-}$).[28] The recipe for polymerization was as follows: deionized water, 1350 cm^3; styrene, 150 g; $NaHCO_3$, 1 g; $K_2S_2O_8$, 1 g; emulsifier, 10 g; temperature, 70 °C. The PBuA particles were prepared in the same way but using sodium dodecyl sulfate (SDS, 2 g) as an emulsifier. Because SDS was used as an emulsifier, the particle sizes of the PBuA particles were larger and their size distribution broader than for the PS particles. The advantage of SDS was its easy removal from the latex. The PS and PBuA particle diameters as measured by quasi-elastic light scattering were 45 and 80 nm, respectively. The size distribution of the PS latex particles was measured by transmission electron microscopy: the number-average and weight-average diameters were 42 and 45 nm.

Heterogeneous Particles with Core−Shell Morphology. PS−PBuA particles having a PS core and a shell made of either PBuA (latex A) or a PBuA-*co*-MAA copolymer (latex B) were synthesized by a two-stage process:[29] A PS particle suspension was first prepared, which was further used as a seed for the polymerization of the shell.

The seed was prepared by a conventional batch emulsion polymerization of styrene at 70 °C using the same recipe as for the homogeneous PS latex described above. But the amount of DDAPS emulsifier was lower (4.5 g), giving larger particle sizes. Quasi-elastic light scattering (QELS) gave a mean diameter of 120 nm, and transmission electron microscopy gave 111 and 114 nm for the number-average and weight-average diameters.

Semibatch seeded polymerizations of shell were then carried out at 70 °C according to the polymerization recipes given in Table 1. Water and the PS seed were first charged into the reactor and heated to the polymerization temperature under nitrogen, the initiator was then added, and the second stage monomer feed (BuA or BuA−MAA mixture) was started at an addition rate of 27 g/h. No additional emulsifier was used. For the MAA-functionalized latex, methacrylic acid was kept as its acidic form since the pH was close to 2 at the end of the polymerization. The conversion followed gravimetrically reached completion. The overall compositions were thus calculated from the polymerization recipes: 40% PS and 60% PBuA for the latex A; 40% PS and 60% PBuA-*co*-MAA which shares into 54.7% BuA and 5.3% MAA for the latex B. The particle sizes (as measured by means of QELS) were 162 nm for sample A and 165 nm for sample B. The ratios of the diameters of the final particles to those of the seed particles were in agreement with the overall composition given by the recipe.

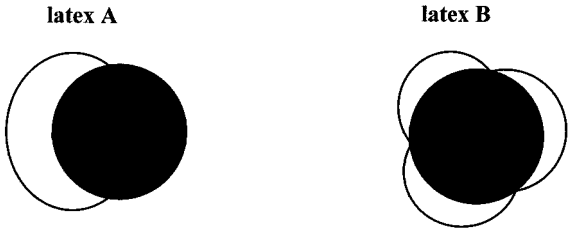

Figure 1. Schematic morphology of composite PS−PBuA particles. Black = PS, white = PBuA or PBuA-*co*-MAA.

Particle Morphology. The morphologies of the two-stage latexes were determined by means of transmission electron microscopy (TEM). The unfunctionalized latex A (PS/PBuA) had clearly not a core−shell morphology. The PBuA part of the particles did not enclose the PS seed, but partial wetting of the PS seed by the PBuA "shell" was observed.[18] The morphology was better defined as a "half-moon" morphology where the coverage of the PS seed was not complete (Figure 1).[29,30] The morphology of the functionalized latex B (PS/PBuA-*co*-MAA) was more complex since TEM revealed a large variety of different morphologies. The overall trend was a more complete coverage of the PS seed than for latex A; many particles were covered by several pieces of PBuA shells. This large set of different morphologies was averaged for the sake of simplicity by the "tree foil" morphology (Figure 1). This kind of morphology results from nonequilibrium wetting conditions during the polymerization.[31]

In every case the latexes were "washed" with a mixture of cationic and anionic ion-exchange resins.[32] This treatment was intended to remove the emulsifier from the latex particles. SDS was easily removed from the latex surface, but the zwitterionic emulsifier DDAPS could not be completely eliminated because of its strong adsorption. An emulsifier having a large adsorption free energy[33] was necessary in order to prepare latex particles of small size and narrow size distribution,[28] but as a counterpart, it was difficult to wash out.

Preparation of the Dry Films. Latex mixtures were prepared by direct mixing of the two colloidal suspensions of PS and PBuA homopolymer latexes. Two compositions were studied, 10 and 45 wt % of PS, below and above the percolation threshold observed by DMA.

Films were cast from the blends or from the suspensions of composite particles A or B, by pouring the required volume (in order to get films of 1 mm thickness) of the colloidal suspension into TEFAL cake molds of 8 cm diameter. The samples were then kept at least 2 weeks for drying in an oven at 313 K (40 °C) under controlled humidity close to the saturated vapor pressure of water. The very slow drying conditions allowed the formation of films of constant thickness which looked homogeneous on a macroscopic scale: they were transparent or slightly turbid. Because of the low T_g of PBuA (−50 °C), PBuA coalescence occurred during the drying process when two PBuA domains contacted each other (Figure 2).

Annealing. A heat treatment of 3 h at 413 K (140 °C), above the glass transition temperature of PS (T_g = 373 K), was applied to samples of each type of film. These samples will be referred to as annealed films in the following.

Methods. *Dynamic Mechanical Analysis*. The mechanical properties of films were estimated from their dynamic elastic and viscous moduli $G'(\omega)$ and $G''(\omega)$. DMA measurements were performed in shear mode at very low strains with a "Micromechanalyser" mechanical spectrometer.[34] Viscoelastic proper-

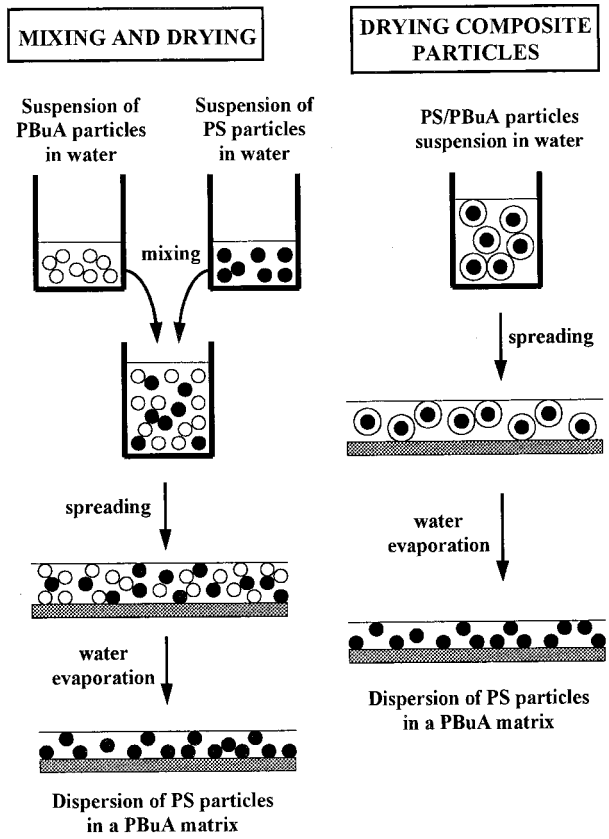

Figure 2. Film formation processes either from mixtures of PS and PBuA particles or from core−shell composite PS/PBuA particles of the types A or B.

ties were measured in the linear regime; the low strain level ($<10^{-4}$) avoided any modification of the film structure during measurements. The present measurements were performed at the fixed frequency of 1 Hz with a 1% accuracy. The elastic modulus of glassy PBuA ($G_0 = 2 \times 10^9$ Pa) was used as a calibration factor for all measurements at low temperatures. This calibration procedure made the correction for small differences of thickness or any other kind of imperfection of the samples.

Small-Angle Neutron Scattering. SANS experiments were carried out with the D11 diffractometer[35] at the high flux reactor of the Institut Laue-Langevin (ILL) at Grenoble. The 1 mm thick films were illuminated with a neutron beam of 1 cm^2 cross section, and the scattered neutrons were collected on a two-dimensional detector with 64 × 64 cells of 1 cm^2 each. The data were radially averaged and normalized for the detector efficiency using the isotropic scattering of a 1 mm thick calibration sample of H_2O. Data reductions were performed with standard procedures available as program packages at the ILL, giving the differential scattering cross section $d\sigma/d\Omega = I(q)$[36] after the subtraction of the incoherent background.

For background subtraction, the background level was estimated such that the q^{-4} decay extended up to the highest q value of the data according to the Porod's asymptotic behavior. The plots of Iq^4 against q^4 were indeed linear for $q > 3 \times 10^{-2}$ Å^{-1}.

The observed scattering vector ($q = (4\pi/\lambda)\sin(\theta/2)$) domains were defined by the wavelength (λ) and the sample-to-detector distance (SD). For the films cast from latex blends containing PS particles of 42 nm diameter, the data collected using two experimental conditions were merged into a single file after the data reduction. The wavelength was $\lambda = 6$ Å, and two SD distances of 20 m (collimation length = 40 m) and 5 m (collimation length = 10 m) were used, giving the experimental q range as 1.5×10^{-3} Å$^{-1} < q < 8 \times 10^{-2}$ Å^{-1}. For films cast from the core−shell latexes with a PS core of 120 nm diameter,

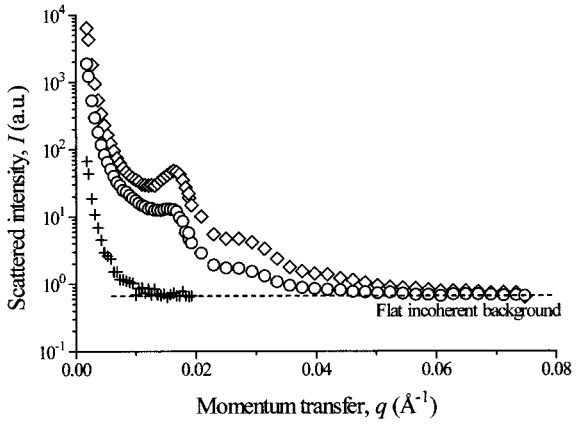

Figure 3. Total scattered intensities (without background subtraction) for films cast from homogeneous particles of pure PBuA (+) and from mixtures of PS and PBuA particles with 10% PS (○) and 45% PS (◇). The pure PBuA sample shows an additional weak scattering at low angle arising from the residual SDS emulsifier. The dashed line shows the level of the incoherent scattering.

$\lambda = 10$ Å, and SD = 35.7 m (collimation distance = 40 m) gave 8×10^{-4} Å$^{-1} < q < 8 \times 10^{-3}$ Å^{-1}.

Neutron Scattering from Latex Films

Scattering from a Dispersion of Particles. Since PBuA coalescence occurs at room temperature, the structure of the films is a dispersion of PS particles in a continuous PBuA matrix. The scattered intensity $I(q)$ for a dispersion of identical particles of number concentration n is the product of a form factor $P(q)$ which depends on the particle morphology and of a structure factor $S(q)$ describing the correlations between PS particles[26,27]

$$I(q) = nP(q)\,S(q) \tag{1}$$

The form factor $P(q)$ for spherical particles of radius R and contrast $\Delta\rho$ with respect to the surrounding medium is

$$P(q) = (\Delta\rho)^2[F(q,R)]^2 = (\Delta\rho)^2[(4\pi/3)R^3 f(qR)]^2$$

with

$$f(x) = 3\,\frac{\sin(x) - x\cos(x)}{x^3} \tag{2}$$

The structure factor $S(q)$ expresses the arrangement of the PS particles in the film. $S(q)$ is the Fourier transform of the pair distribution function $g(r)$.

In the theoretical calculations of the scattered intensity, the influence of the size distribution was accounted for by means of a Schulz distribution of radii.[37] The smearing caused by the wavelength dispersion ($\Delta\lambda/\lambda$ = 9%) and geometrical resolution effects were also taken into account.[38]

Contrast Conditions. A favorable contrast (i.e., a difference of coherent scattering length densities) between the PS particles and the PBuA matrix was obtained with natural isotopic compositions, avoiding the use of deuterated materials. This unusual choice is often considered as unfavorable for SANS experiments because hydrogen atoms (^{1}H) produce a large incoherent scattering which may hide the coherent scattering. The present coherent scattering was strong enough for being larger than the incoherent background (Figure 3), so

Table 2. Scattering Length Densities of Compounds Found in Dry Films

compound	scattering length density ρ (cm^{-2})	contrast $\Delta\rho$ (cm^{-2})
PBuA(^{1}H)	0.66×10^{10}	
PS(^{1}H)	1.40×10^{10}	0.74×10^{10}
PS(^{2}H)	6.42×10^{10}	5.76×10^{10}
DDAPS emulsifier	0.08×10^{10}	0.58×10^{10}

that the background subtraction was accurate.

Multiple scattering occurred under such contrast conditions because of the strong incoherent scattering. The transmissions of the samples were indeed close to 50%. The transmissions were also close to that of pure PBuA, showing that incoherent scattering was predominant. Multiple scattering did not distort the data because of the predominance of incoherent scattering. The largest part of the multiple scattering included an incoherent scattering event and was thus isotropic; the probability for a fully coherent multiple scattering event was very low. The neutrons that were scattered several times were a part of the flat incoherent background.

The scattering length densities and contrasts $\Delta\rho = |\rho - \rho_{PBuA}|$ of hydrogenated PS and PBuA are given in Table 2, together with the scattering length density of deuterated polystyrene given for comparison. A higher contrast would be obtained if deuterated PS was used. The increase of $\Delta\rho$ by a factor of 8 would result in an increase of the coherent scattering by a factor of 60 ($I \propto (\Delta\rho)^2$), but the thickness of the samples should then be reduced in order to avoid coherent multiple scattering. The use of protonated materials allowed the SANS measurements with the same 1 mm thick films as those used for DMA.

Results and Discussion

Films Cast at Room Temperature from Mixtures of PS and PBuA Particles. Elastic moduli G' measured by means of DMA as a function of temperature[18b] show two drops of moduli at the glass transition temperatures of PBuA and PS. G' strongly depended on the PS content in the temperature domain between the two T_g where PBuA was in its rubber state while PS was glassy. For PS volume fractions below 30%, elastic moduli were so low ($G' \approx 10^5$ Pa) that they could not be measured with the mechanical spectrometer. G' increased with the PS content (Figure 4a) above this volume fraction which was identified as the percolation threshold. Annealing the films at 140 °C for 3 h resulted in a further increase of elastic moduli (Figure 4b). Efficient mechanical reinforcement involves a percolating network of PS particles that are stuck by any mechanism. For films cast at room temperature, the nature of the "bonds" and the extent of the contact area between PS particles appear as key parameters in the control of the mechanical properties. These are local structural details to be studied by means of a local method of investigation such as SANS. On the same footing, the structural transformations brought out by the thermal treatments were investigated at a local scale by SANS.

The structure of two dry films below and above the percolation threshold has been investigated by means of SANS. The SANS data for films with 10% and 45% PS contents (Figure 5) looked similar although these compositions were located below and above the percolation threshold determined by DMA. Going from the high-q region (high resolution) to the low-q one, three

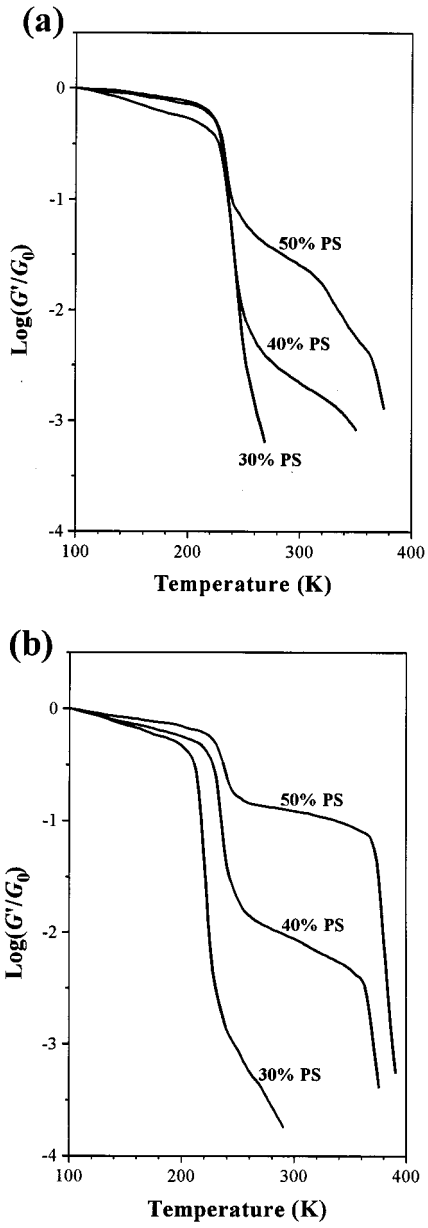

Figure 4. Elastic modulus of films cast at room temperature from PS−PBuA latex blends as a function of temperature for different PS volume fractions:[18] (a) as-dried films; (b) films annealed at 140 °C for 3 h.

characteristic behaviors were observed: the asymptotic q^{-4} decay of scattered intensity, a broad peak around 0.015−0.02 $Å^{-1}$, and a strong rise of scattered intensity at low angles. These three parts of the data corresponding to different q ranges will be discussed successively in the following.

(1) In the high-q domain extending above 0.02 $Å^{-1}$, the scattered intensity decays as q^{-4} according to the asymptotic Porod's law

$$I(q) = 2\pi(\Delta\rho)^2 A/V q^{-4} = K_{Prd} q^{-4} \qquad (3)$$

where A/V is the interfacial area (A) per unit sample volume (V). There was no q^{-2} decay that the emulsifier adsorbed at the PS−PBuA interface would give.[8] The scattering at high q is that of a sharp interface separating PS and PBuA; their is no mixing region between PS and PBuA according to the experimental resolution of 10 Å. PS and PBuA are indeed immiscible polymers.

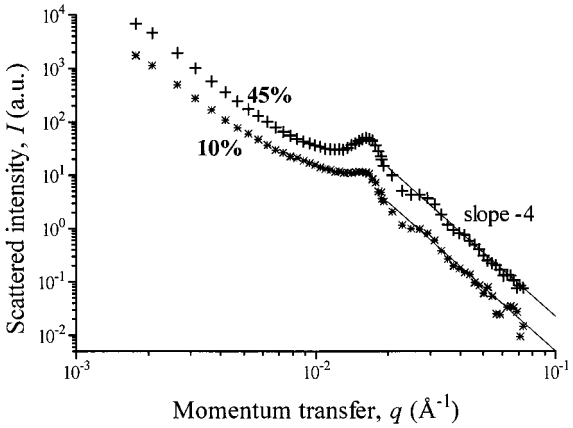

Figure 5. Scattered intensity for films with 10% and 45% PS content dried at room temperature (log−log scale).

The interfacial area A is given by the value of the prefactor in Porod's law. The interfacial area ratio $A(45\%)/A(10\%) = 4.5$ has been retained in the dry film. No coalescence of PS particles could occur during the film formation at room temperature.

The diameter of the PS particles was calculated from the oscillations about the Porod asymptote in the high-q domain where $S(q) \approx 1$. The best fit of eq 2 to the experimental data (Figure 6a for $q > 0.02$ Å^{-1}) gave a mean diameter of 42 nm with a good precision and a rough estimate of the width of the size distribution as $\sigma/D \approx 10\%$. The z-average diameter calculated from the Schulz size distribution was 44 nm, in agreement with the value measured by quasi-elastic light scattering (45 nm).

(2) A peak (hump) was observed at $q = 0.0165$ Å^{-1} for both the films having 10% and 45% PS content. It is related to the correlations between PS particles giving an interparticle structure factor $S(q)$. This peak has nothing to do with the form factor of the PS particles since the first maximum of $P(q)$ for spheres having 42 nm diameter is located at $q = 0.0275$ Å^{-1}. (The first maximum of eq 2 occurs at $qR = 5.765$.)

According to the experimental resolution, this peak was too broad for being a Bragg peak. The PS particles ordering was not periodic. If the dispersion of PS particles throughout the film was at random, the mean distance between PS particles would be larger, and the peak would be located at lower q, for films with 10% PS content than for 45%. Moreover, the peak was observed at a higher q than predicted for a random dispersion of 42 nm diameter particles at 45% volume fraction (Figure 6b). As a conclusion, the PS particles were not distributed at random. The separation between PS particles was shorter than for a random distribution, which meant that the PS particles were aggregated into clusters. The structure of the film was made of regions that were enriched in PS particles, at the expense of remaining regions containing less PS particles than the average value.

The important observation was that the peak position was identical at 10% and 45% PS contents, indicating that the composition of the clusters was the same, whatever the overall composition. This behavior has the same features as a phase separation. A macroscopic phase separation did not occur; however, the films were optically transparent.

(3) The strong rise of the scattered intensity at low angles ($q < 10^{-2}$ Å^{-1}) may arise either from the form

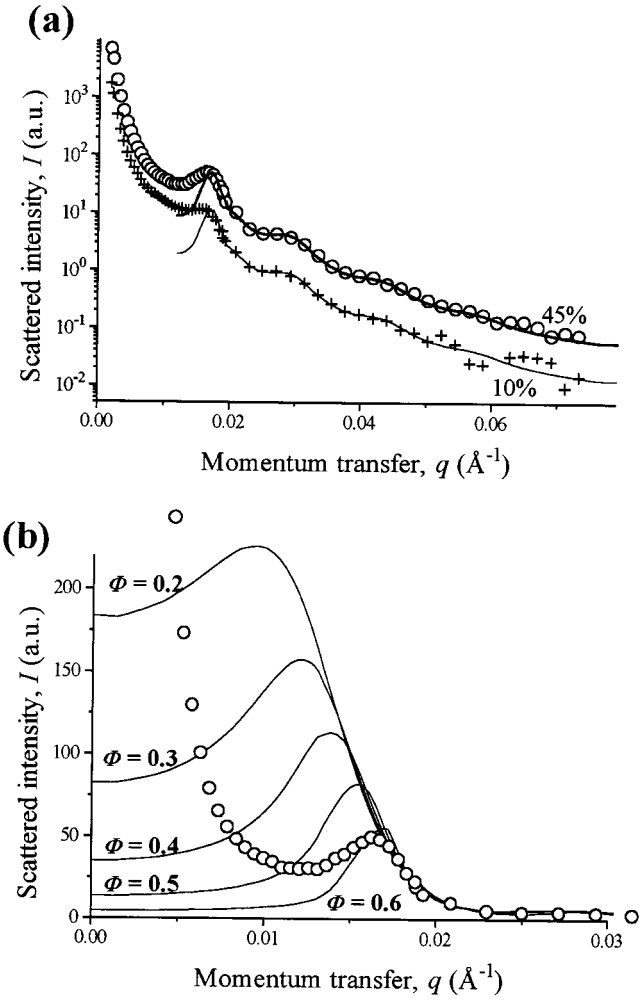

Figure 6. (a) $I(q)$ for the films containing 45% (○) and 10% (+) of PS and the corresponding calculated spectra (solid lines). (b) $I(q)$ for the 45% PS content film with the theoretical predictions of the model of phase separation of hard-sphere clusters for different volume fractions Φ inside the clusters (solid lines).

factor of the clusters or from large lumps where the residual emulsifier has been expelled to. On one hand, the clusters may contribute to the scattering for $10^{-3} < q < 10^{-2}$ Å^{-1} if their size remains moderate. On the other hand, the segregation of residual emulsifier into large lumps in homogeneous polymer films gave the same characteristic low-q rise of scattered.[8] Such pools of pure emulsifier having diameters of several micrometers could be observed by means of electron microscopy.[39] It was not possible to ascertain the origin of the low-angle scattering from the present data. The scattering below 10^{-2} Å^{-1} will not be discussed further in this paper.

Since the aggregation phenomenon resembled so closely a phase separation at the scale of SANS, it was modeled as a two-phase separation: the coexistence of clusters of PS particles immersed in a continuous matrix of PBuA and regions containing pure PBuA. Within this model, the scattering is the sum of the scattering from the clusters containing a volume fraction Φ of PS and of the flat and weak scattering of the remaining pure PBuA domains. The peak position and shape contain the information on the internal structure of the clusters, that is, their PS volume fraction and the ordering of the PS particles inside the clusters. A calculation assuming a random distribution of the PS particles[40] inside the

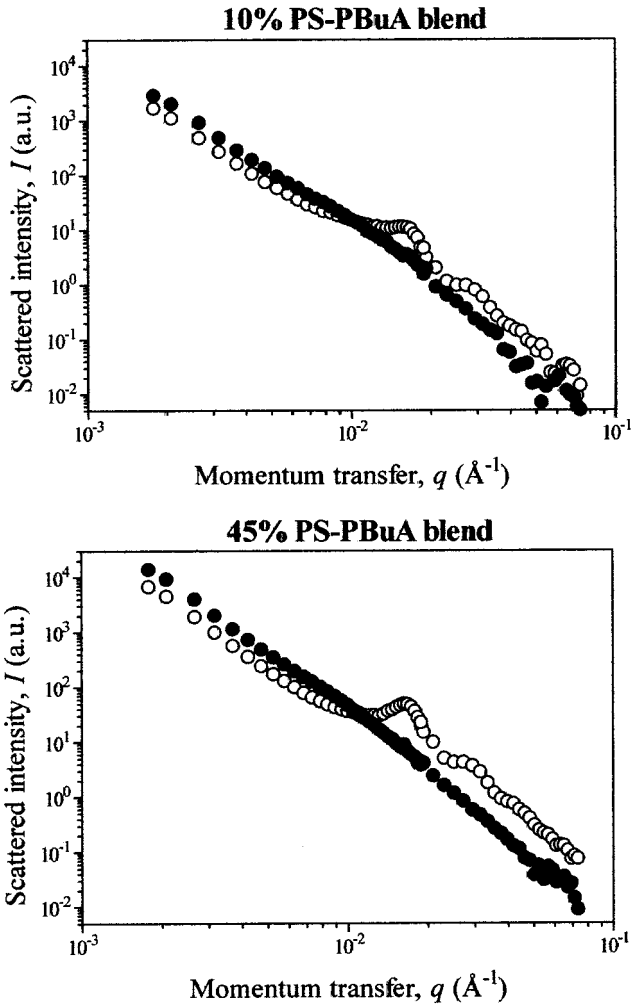

Figure 7. Influence of annealing on SANS data for the films containing 10% (left) and 45% (right) of PS: (○) as-dried films; (●) after annealing at 140 °C for 3 h.

clusters gave a satisfactory account of the experimental data for $\Phi = 60\%$ (Figure 6a, solid line). The position of the peak is quite sensitive to the value of Φ (Figure 6b). The model also accounted quite well for the shape of the peak at its high-q side where it was not altered by the low-angle scattering. The model could predict the peak position (Φ was adjusted for that), but also the width of the peak without any additional fitting parameter. The arrangement of PS particles inside the clusters was thus close to random. The volume fraction of PS inside the dense clusters was the same for both samples since the position of the peak was the same.

Films of Mixtures of PS and PBuA Particles after Thermal Annealing above the T_g of PS. The films described above were annealed for 3 h at 140 °C in order to allow coalescence of the PS particles. This thermal treatment resulted in a considerable reinforcement of mechanical properties (Figure 4).

Annealing led to a loss of the PS−PS correlation peak in the scattering data (Figure 7). Coalescence of PS particles occurred in both samples (10% and 45% PS content), giving rise to larger PS nodules. Porod's law was still followed at high q, showing that there was no mixing of PS and PBuA upon annealing. The PS−PBuA interfacial area as measured from Porod's law (eq 3) was reduced upon annealing by a factor of 2.8 and 5.0 for the films with 10% and 45% PS contents, respectively. Assuming that N PS particles merge into a single sphere

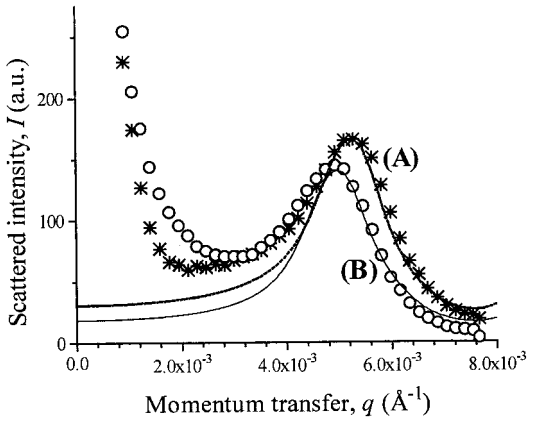

Figure 8. SANS data for films A and B compared with the predictions for the models as described in the text. Sample A (experimental, ○; calculated, dashed line); sample B (experimental, *; calculated, solid line).

containing pure PS, simple geometry implies $(K_{Prd})_{as-dried}/(K_{Prd})_{annealed} = N^{1/3}$, giving $N = 20$ below the percolation threshold (10% PS content).

Films Obtained at Room Temperature from Composite PS/PBuA Particles. The films cast from the core−shell particles A and B contained both 40% of PS, which was above the percolation threshold of the blends. As for the films cast from latex mixtures described above, a broad peak and an intensity rise at small q could be observed. The q range was not large enough toward high q for observing the expected Porod's q^{-4} decay. The strong scattering at small angle was again ignored in the discussion. The spatial ordering of the PS particles was analyzed in the same way as for the blends.

For sample A, the model of phase separation with a random distribution of particles inside the clusters gave the correct peak position and shape for an internal PS volume fraction of 48% (Figure 8), close to the overall PS volume fraction of 40%. The core−shell structure of the particles has prevented to a large extent the aggregation of the PS particles.

Conversely, this model could not fit accurately to the experimental data for sample B. A random distribution of PS particles at 40% volume fraction (equal to the overall composition) gave the correct peak position, but the observed peak was sharper. The peak sharpening was ascribed to the protective coating coming from the PBuA-*co*-MAA shell, ensuring a better coverage than in sample A. A shell around the PS spheres from where other PS particles are excluded gives a more ordered structure. A model with PS spheres having their true diameter of 120 nm surrounded by an excluded shell is proposed. This is still a hard-sphere model,[40] but the excluded volume is larger than the actual volume of each particle. (The hard-sphere diameter exceeds the particle diameter.) Taking the diameter of the particles (120 nm) and the PS volume fraction (40%) as fixed parameters, the best fit to the experimental data was found for an excluded shell of 4 nm thickness (Figure 8). This is much less than the 22 nm mean shell thickness of the particles as calculated from their overall chemical composition.

The core−shell morphology of the particles prevented the PS core aggregation into PS-rich clusters. The better the coverage of the glassy core by the soft shell, the more efficient this inhibition. The model used for film B would mean complete inhibition of the aggregation since the

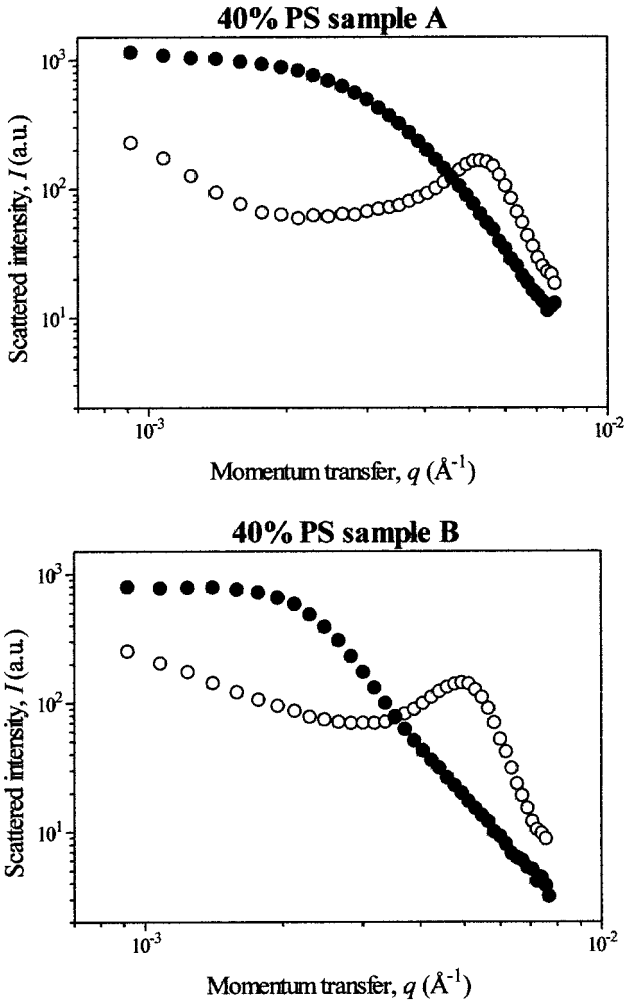

Figure 9. SANS data before (○) and after (●) annealing for samples A and B.

excluded volume around each core prohibits the direct contacts between PS cores. This is a phenomenological model, and the small thickness of the excluded shell is an effective value, so that some contacts between PS cores actually may exist. As a more realistic picture, a partial coverage of the PS cores by a PBuA shell defines an excluded area for other PS cores. The consequence of this partial "poisoning" of the PS area was a reduction of the connectivity in building clusters of PS particles. This phenomenon switched the structure from a percolating network to a nonpercolating one for a given overall PS content.

Films of Composite PS/PBuA Particles after Thermal Annealing above the T_g of PS. Annealing resulted in the disappearance of the peak as for the films cast from blends. In contrast with PS−PBuA blends, the scattered intensity from the annealed films did not diverge at low q but leveled off toward the low-q values, showing that the PS domains were of limited sizes (Figure 9). The sizes of the PS domains after coalescence followed closely the extent of aggregation of PS particles in the films dried at room temperature.

As a consequence, drastic differences in mechanical properties were observed for the films cast from blends and core−shell particles; the elastic modulus increased with the extent of aggregation of the PS particles (Figure 10). For sample B, the measured moduli were close to that of pure PBuA because the core−shell structure separated efficiently the PS cores. This clearly

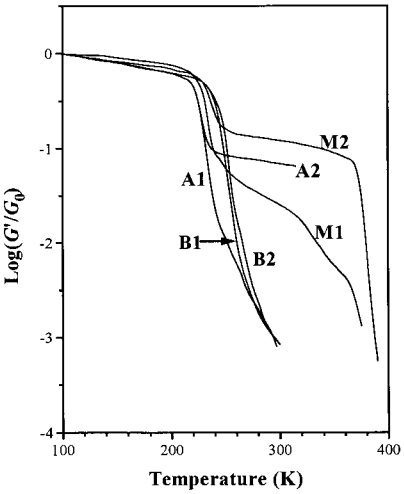

Figure 10. Elastic moduli of films from a PS−PBuA mixture with 50% PS content (M) and from the PS/PBuA core−shell latexes A and B as a function of temperature in their as-dried state (M1, A1, and B1) and after annealing at 140 °C for 3 h (M2, A2, and B2).

shows that a large area of contact between PS particles is necessary for the building up of large continuous glassy domains. The effect of annealing on mechanical properties was less for sample A having an imperfect core−shell morphology than for the blends because of the inhibition of the coalescence by the PBuA shell. PS coalescence requires contacts between PS particles in the initial dry film.

Discussion

We have shown by SANS that the PS particles aggregate into clusters in films cast from blends, whereas the aggregation was prevented in the case of latex particles with a core−shell morphology. A high mechanical reinforcement was attained with the blends, and annealing above the T_g of PS provided a supplementary improvement of the mechanical properties. On the contrary, the influence of the PS cores acting as fillers was quite low in the case of core−shell particles. The way the PS particles were mixed with the PBuA matrix has a strong influence on the structure and mechanical properties of the films. The amount of PS coalescence and the associated mechanical reinforcement upon thermal treatment were also related to the mixing process.

The aggregation of the PS particles appears as a key parameter, and the following relationship between the film structure and the mechanical properties emerges out of this study. In the films where extensive PS aggregation takes place, the high density of contacts between the PS particles in the as-dried films induces a percolating network of PS and allows the fast coalescence of PS upon thermal treatments.

Some basic questions deserve further discussion in light of the present findings: What is the mechanism of aggregation, and why does the core−shell morphology prevent the aggregation? Could the aggregation reach the macroscopic phase separation between the immiscible PS and PBuA polymers? What is the microscopic origin of the mechanical reinforcement? What kind of interaction does link the PS particles in building up a percolating network?

The Mechanism of Aggregation. There are few experimental observations of such a segregation phe-

nomenon of hard particles in a soft film. Eckersley and Helmer[20] provided evidence of the formation of clusters of hard particles by means of electron microscopy. They also could show the segregation of the hard particles at the surface of the film, as was already observed by atomic force microscopy.[41,42]

The film formation can be described by an out-of-equilibrium process where particles are frozen in by the coalescence of PBuA parts during the formation of a dry film. As the particles approach each other during drying, the system undergoes a transition from a dispersed state where the particles are surrounded by the solvent to a condensed state (film) where the rubber parts of the particles have coalesced.

The late stage of the drying process is the coexistence of a colloidal suspension and a dry film, the dry film "phase" growing at the expense of the colloidal suspension.[8] The formation of a film appears as a transition driven by the loss of the colloidal stability of the particles. The flocculation of one or the other type of particle in a mixture should occur according to their colloidal stability. Two scenarios can be devised: either PS particles flocculation occurred sooner than that of PBuA ones or the reverse. Both processes lead to a segregation of PS and PBuA particles. The interaction between particles depends on their size and electrical charge. If each macromolecule bears two sulfate groups coming from the potassium persulfate initiator (one at each macromolecular chain end), larger particles having a larger electrical charge are more stable. The aggregation of smaller particles resulting from their weaker electrostatic stabilization has indeed been observed.[43] In the case of mixtures of hard spheres, the expected phase separation of the largest particles caused by the osmotic pressure of the smaller ones has been observed for PMMA particles dispersed in decalin.[44] The prediction of the colloidal stability on simple grounds is then a difficult task. Careful appraisal of the colloidal stability (by measurements of partial structure factors) and observation of the drying kinetics would be necessary. One can speculate that mixtures of particles having the same colloidal stability (i.e., the same size and electrical charge) would lead to the formation of a dry film with a random distribution of glassy particles in the rubber matrix.

In the case of blends, clusters of PS particles having an internal PS volume fraction of 60% were formed, whatever the composition of the initial colloidal suspension. This is close to the maximum volume fraction allowed for a disordered (nonperiodic) dense packing of spherical particles.[45] A denser packing into an ordered array would leave interstices between the spherical PS particles to be filled by small enough PBuA particles. If such small particles cannot be found in the size distribution of the PBuA particles, the aggregation stops. The formation of voids between the PS particles is unlikely because of the interfacial free energy cost. The massive formation of voids was ruled out because the films were optically transparent. The maximum volume fraction of glassy particles that a rubber film can accommodate, while retaining its rubber properties, was found experimentally between 50 and 55%.[20,46,47] The films get turbid and brittle above it because of the formation of cracks during the film formation process.[46−48]

The Relationship between Mechanical Properties and Structure. According to the present findings,

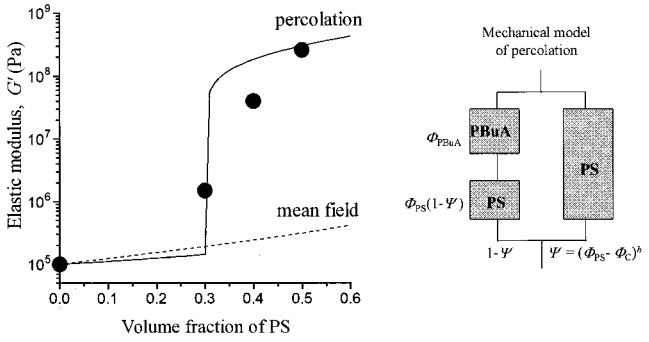

Figure 11. Shear modulus (real part) as a function of the volume fraction of PS. Black circles: experimental data at 280 K for annealed films. The model calculations were performed taking the elastic moduli of pure PS and PBuA as $G'_{PS} = 10^9$ Pa and $G'_{PBuA} = 10^5$ Pa. Full line: percolation model with $\Phi_C = 0.30$ and $b = 0.4$. Dashed line: mean field approach (Kerner[15,49] with $\mu_{PBuA} = 0.33$). The phenomenological mechanical model for the percolation is shown on the right.

the aggregation of the PS particles has a drastic influence on the mechanical properties, but the detailed origin of the mechanical reinforcement deserves a further discussion. The important point is that the influence of the aggregation manifests only above the percolation threshold, although it is also present at lower PS contents.

The reinforcing effect of PS particles was much higher than predicted on the basis of mean field theories.[15,49] On the contrary, it is worth noting that the reinforcement was negligible below a volume fraction of 30%, which was identified as the percolation threshold. The skeleton formed by the percolating tree of rigid particles was at the origin of the reinforcing effect. It is strongly nonlinear, following the PS content of the percolating network.[18c,d] The volume fraction Ψ of PS involved in the continuous branches of the percolating tree follows a scaling law such as $(\Phi_{PS} - \Phi_C)^b$, Φ_C being the percolation threshold and b the exponent corresponding to the property (here the shear modulus).[50] An estimate of b is 0.40.[51,52] The experimental data and the predictions of the Kerner equation[49] and of the percolation model[18c,d] are compared in Figure 11. The percolation gives the correct order of magnitude in the annealed films. It should be noticed that the percolation model allows a direct calculation of the elastic modulus from the properties of the pure phases and the value of the percolation threshold; there is no free parameter that could be used in looking for the best fit to the experimental data.

Strong links should stick the PS particles for the percolating network to be rigid. In previous works reporting the high reinforcing effects of cellulose whiskers dispersed in a soft matrix,[18d] the stiffness of the percolating network of whiskers resulted from the ability of cellulose to form hydrogen bonds. In the present work, the coalescence of PS particles above T_g should play a similar role.

The adhesion between PS particles in the as-dried films is less powerful since the elastic moduli were lower than for the annealed films. There was also a noticeable temperature dependence which suggested the presence of thermally activated phenomena. The PS particles may be either at direct contact or linked through a thin immobilized layer of PBuA between them. This latter idea was put forward by Eisenberg[53] as a possible origin of the mechanical properties of ionomers: ionic multi-

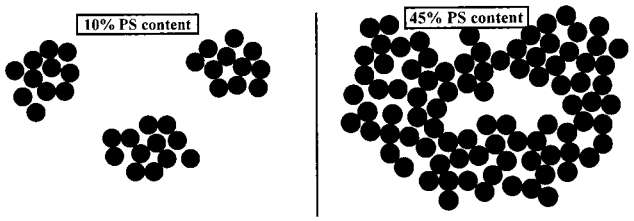

Figure 12. Sketch of the structure of the films of blends with 10% and 45% PS content.

plets aggregate into clusters where the mobility of the polymer is reduced; a percolating network of clusters ensures the elasticity of the materials. This idea was extended to the dispersion of small silica particles (7 nm diameter) in a rubber matrix.[53c] A transition at a temperature higher than T_g was ascribed to the layer of immobilized polymer in the vicinity of the ionic multiplets or silica particles. For very small particles, the layer of immobilized polymer (1 nm thick) makes a large fraction of the rubber matrix because of the large specific area of the fillers. Such a transition was not observed in latex films because the particles were of larger size. This layer does exist, however: NMR relaxation[54−57] and nonradiative energy transfer experiments[58,59] have shown the presence of a polymer layer of reduced mobility at the vicinity of the interface.

The percolating network has to be free of defects; that is, each particle should be able to make at least two efficient links with its direct neighbors. The density of contacts between the particles determines the mechanical properties: a high density of contact ensures the formation of a continuous domain of PS. The local structure at the nanometer scale controls the macroscopic mechanical properties. A high density of contacts between PS particles is also important for the coalescence of PS during annealing. The results on the films cast from core−shell latexes showed that it was not necessary to invoke the formation of new contacts during annealing. The clusters of coalesced PS particles remained of finite size because the low density of contacts and percolation did not take place; the mechanical reinforcement was poor.

Conclusions

In composite films made of PS particles of high T_g embedded in a PBuA matrix of low T_g, the dispersion of the PS particles is not random and depends drastically on the way PS particles were brought into the films.

In films cast from mixtures of PS and PBuA particles, the aggregation of the PS particles into clusters took place, even for the low PS volume fraction of 10%. Clusters of PS particles having a high density ($\Phi = 60\%$) were formed, whatever the overall PS content (Figure 12). The aggregation phenomenon looked like a phase separation that has been quenched at a nonequilibrium colloidal state during drying. A model of phase separation between a PS-rich phase containing a PS volume fraction of 60% and pure PBuA accounted for the SANS data.

The aggregation could be prevented by the use of composite particles with a core−shell morphology. SANS and DMA measurements were consistent with the presence of a thin PBuA protective coating around the PS particles that inhibited the direct contacts between PS particles.

Large elastic moduli were obtained when extensive PS−PS contacts in the films dried at room temperature led to a percolating network of PS particles. Strong mechanical reinforcement could be achieved by heating the dry films above the PS T_g if the PS particles coalescence was allowed in the as-dried films structure: PS−PS particles contacts were required for fast coalescence to occur during annealing. A PS surface area loss could be observed during coalescence.

Since a high density of contacts was required for setting up the percolation, the aggregation of the PS particles during the film formation process was a benefit. The advantage of using latexes with a core−shell morphology was a better "mixing" of the immiscible polymers in the dry films, but this occurred at the expense of the mechanical properties. A nonuniform distribution of the PS particles does not mean that the film is ill-defined or sloppy, but this aggregation phenomenon has to be carefully controlled. A macroscopic phase separation would lead to irreproducible properties, cracks in domains where the PS enrichment would be excessive.

The combined use of macroscopic (DMA) and local (SANS) investigation methods allows to progress in the understanding of the mechanisms of film formation. The present study provides a methodology that could be applied to more systematic studies about composite films. In particular, SANS allows the measurement of the interfacial area loss during coalescence. Mechanical measurements and structural studies by SANS could be carried out on the same samples of 1 mm thickness without any specific deuteration.

References and Notes

(1) Warson, H. *The Applications of Synthetic Resin Emulsions*; Ernest Benn Ltd: London, 1972.
(2) Lovell, P. A., El-Aasser, M. S., Eds. *Emulsion Polymerization and Emulsion Polymers*; Wiley: New York, 1997.
(3) Bradford, E. B.; Vanderhoff, J. W. *J. Macromol. Chem.* **1966**, *1*, 335.
(4) Bradford, E. B.; Vanderhoff, J. W. *J. Macromol. Sci. Phys.* **1972**, *B6*, 671.
(5) Vanderhoff, J. W.; Bradford, E. B.; Carrington, W. K. *J. Polym. Sci., Polym. Symp.* **1973**, *41*, 155.
(6) Provder, Th., Winnik, M., Urban, M., Eds. *Film Formation in Waterborne Coatings*; *ACS Symp. Ser.* **1996**, *648*.
(7) Keddie, J. L. *Mater. Sci. Eng.* **1997**, *R21*, 101.
(8) (a) Joanicot, M.; Wong, K.; Maquet, J.; Chevalier, Y.; Pichot, C.; Graillat, C.; Lindner, P.; Rios, L.; Cabane, B. *Prog. Colloid Polym. Sci.* **1990**, *81*, 175. (b) Chevalier, Y.; Pichot, C.; Graillat, C.; Joanicot, M.; Wong, K.; Maquet, J.; Lindner, P.; Cabane, B. *Colloid Polym. Sci.* **1992**, *270*, 806.
(9) Zosel, A.; Ley, G. *Prog. Colloid Polym. Sci.* **1996**, *101*, 86.
(10) (a) Hahn, K.; Ley, G.; Schuller, H.; Oberthür, R. *Colloid Polym. Sci.* **1986**, *264*, 1092. (b) Hahn, K.; Ley, G.; Oberthür, R. *Colloid Polym. Sci.* **1988**, *266*, 631.
(11) (a) Yoo, J. N.; Sperling, L. H.; Glinka, C. J.; Klein, A. *Macromolecules* **1990**, *23*, 3962. (b) Yoo, J. N.; Sperling, L. H.; Glinka, C. J.; Klein, A. *Macromolecules* **1991**, *24*, 2868. (c) Kim, K. D.; Sperling, L. H.; Klein, A.; Wignall, G. D. *Macromolecules* **1993**, *26*, 4624. (d) Kim, K. D.; Sperling, L. H.; Klein, A.; Hammouda, B. *Macromolecules* **1994**, *27*, 6841.
(12) Joanicot, M.; Wong, K.; Cabane, B. *Macromolecules* **1996**, *29*, 4976.
(13) Pekcan, Ö. *Trends Polym. Sci.* **1994**, *2*, 236.
(14) Dickie, R. A. *J. Appl. Polym. Sci.* **1973**, *17*, 45, 65, 79.
(15) Paul, D. R.; Newman, S. *Polymer Blends*; Academic Press: New York, 1978.
(16) Rynders, R. M.; Hegedus, C. R.; Gilicinski, A. G. *J. Coat. Technol.* **1995**, *67*, 59.
(17) Winnik, M. A.; Feng, J. *J. Coat. Technol.* **1996**, *68*, 39.
(18) (a) Cavaillé, J.-Y.; Pérez, J. *Makromol. Chem., Macromol. Symp.* **1990**, *35/36*, 405. (b) Cavaillé, J.-Y.; Vassoille, R.; Thollet, G.; Rios, L.; Pichot, C. *Colloid Polym. Sci.* **1991**, *269*, 248. (c) Ouali, N.; Cavaillé, J.-Y.; Pérez, J. *Plast., Rubber*

Compos. Process. Appl. **1991**, *16*, 55. (d) Favier, V.; Chanzy, H.; Cavaillé, J.-Y. *Macromolecules* **1995**, *28*, 6365.
(19) Carreau, P. J.; Lavoie, P.-A.; Bagassi, M. *Macromol. Symp.* **1996**, *108*, 111.
(20) Eckersley, S. T.; Helmer, B. J. *J. Coat. Technol.* **1997**, *69* (864), 97.
(21) (a) Payne, A. R. *Rubber Plast. Age* **1961**, 963. (b) Payne, A. R.; Whittaker, R. E. *Rubber Chem. Technol.* **1971**, *44*, 440.
(22) Medalia, A. I. *Rubber Chem. Technol.* **1978**, *51*, 437.
(23) (a) Hidalgo, M.; Cavaillé, J.-Y.; Guillot, J.; Guyot, A.; Pichot, C.; Rios, L.; Vassoille, R. *Colloid Polym. Sci.* **1992**, *270*, 1208. (b) Hidalgo, M.; Cavaillé, J.-Y.; Cabane, B.; Chevalier, Y.; Guillot, J.; Rios, L.; Vassoille, R. *Polym. Adv. Technol.* **1995**, *6*, 296.
(24) Cavaillé, J.-Y.; Jourdan, C.; Kong, X. Z.; Perez, J.; Pichot, C.; Guillot, J. *Polymer* **1986**, *27*, 693.
(25) (a) Zosel, A.; Heckmann, W.; Ley, G.; Mächtle, W. *Colloid Polym. Sci.* **1987**, *265*, 113. (b) Zosel, A.; Heckmann, W.; Ley, G.; Mächtle, W. *Makromol. Chem., Macromol. Symp.* **1990**, *35/36*, 423.
(26) Lindner, P., Zemb, Th., Eds. *Neutron, X-ray and Light Scattering: Introduction to an Investigative Tool for Colloidal and Polymeric Systems*; North-Holland: Amsterdam, 1991.
(27) Chevalier, Y. *Trends Polym. Sci.* **1996**, *4*, 197.
(28) Essadam, H.; Pichot, C.; Guyot, A. *Colloid Polym. Sci.* **1988**, *266*, 462.
(29) Rios, L.; Hidalgo, M.; Cavaillé, J.-Y.; Guillot, J.; Guyot, A.; Pichot, C. *Colloid Polym. Sci.* **1991**, *269*, 812.
(30) (a) Chen, Y.-C.; Dimonie, V. L.; El-Aasser, M. S. *Pure Appl. Chem.* **1992**, *64*, 1691. (b) Chen, Y.-C.; Dimonie, V. L.; Shaffer, O. L.; El-Aasser, M. S. *Polym. Int.* **1993**, *30*, 185.
(31) Rudin, A. *Macromol. Symp.* **1995**, *92*, 53.
(32) Van den Hul, H. J.; Vanderhoff, J. W. *J. Colloid Interface Sci.* **1968**, *28*, 336.
(33) Graillat, C.; Dumont, B.; Depraetere, P.; Vintenon, V.; Pichot, C. *Langmuir* **1991**, *7*, 872.
(34) Étienne, S.; Cavaillé, J.-Y.; Perez, J.; Point, R.; Salvia, M. *Rev. Sci. Instrum.* **1982**, *53*, 1261.
(35) (a) Lindner, P.; May, R. P.; Timmins, P. A. *Physica B* **1992**, *180*, 967. (b) http://www.ill.fr/YellowBook/.
(36) Cotton, J.-P. In *Neutron, X-ray and Light Scattering: Introduction to an Investigative Tool for Colloidal and Polymeric Systems*; Lindner, P., Zemb, Th., Eds.; North-Holland: Amsterdam, 1991; p 19.
(37) Hayter, J. B. In *Physics of Amphiphiles: Micelles, Vesicles and Microemulsions*; Degiorgio, V., Corti, M., Eds.; North-Holland: Amsterdam, 1985; p 59.
(38) Pedersen, J. S.; Posselt, D.; Mortensen, K. *J. Appl. Crystallogr.* **1990**, *23*, 321.
(39) Richard, J.; Maquet, J. *Polymer* **1992**, *33*, 4164.
(40) Ashcroft, N. W.; Lekner, J. *Phys. Rev.* **1966**, *145*, 83.
(41) Butt, H.-J.; Kuropka, R. *J. Coat. Technol.* **1995**, *67*, 101.
(42) Patel, A. A.; Feng, J.; Winnik, M. A.; Vancso, G. J.; Dittman McBain, C. B. *Polymer* **1996**, *37*, 5577.
(43) Ottewill, R. H.; Hanley, H. J. M.; Rennie, A. R.; Straty, G. C. *Langmuir* **1995**, *11*, 3757.
(44) Bartlett, P.; Ottewill, R. H.; Pusey, P. N. *J. Chem. Phys.* **1990**, *93*, 1299.
(45) Bennett, C. H. *J. Appl. Phys.* **1972**, *43*, 2727.
(46) Feng, J.; Winnik, M. A.; Shivers, R. R.; Clubb, B. *Macromolecules* **1995**, *28*, 7671.
(47) Lepizzera, S.; Lhommeau, C.; Dilger, G.; Pith, T.; Lambla, M. *J. Polym. Sci., Part B: Polym. Phys.* **1997**, *35*, 2093.
(48) (a) Keddie, J. L.; Meredith, P.; Jones, R. A. L.; Donald, A. M. *Macromolecules* **1995**, *28*, 2673. (b) Keddie, J. L.; Meredith, P.; Jones, R. A. L.; Donald, A. M. *Langmuir* **1996**, *12*, 3793.
(49) Kerner, E. H. *Proc. Phys. Soc.* **1956**, *69B*, 808.
(50) Stauffer, D. *Introduction to Percolation Theory*; Taylor & Francis: London, 1985.
(51) Kirkpatrick, S. *Rev. Mod. Phys.* **1973**, *45*, 574.
(52) de Gennes, P.-G. *Scaling Concepts in Polymer Physics*; Cornell University Press: Ithaca, NY, 1979.
(53) (a) Eisenberg, A.; Hird, B.; Moore, R. B. *Macromolecules* **1990**, *23*, 4098. (b) Kim, J.-S.; Jackman, R. J.; Eisenberg, A. *Macromolecules* **1994**, *27*, 2789. (c) Tsagaropoulos, G.; Eisenberg, A. *Macromolecules* **1995**, *28*, 6067.
(54) Hidalgo, M.; Guillot, J.; Llauro-Darricades, M.-F.; Waton, H.; Pétiaud, R. *J. Chim. Phys.* **1992**, *89*, 505.
(55) Tembou-Nzudie, D.; Delmotte, L.; Riess, G. *Macromol. Chem. Phys.* **1994**, *195*, 2723.
(56) Nelliappan, V.; El-Aasser, M. S.; Klein, A.; Daniels, E. S.; Roberts, J. E. *J. Appl. Polym. Sci.* **1995**, *58*, 323.
(57) (a) Landfester, K.; Boeffel, C.; Lambla, M.; Spiess, H. W. *Macromol. Symp.* **1995**, *92*, 109. (b) Landfester, K.; Boeffel, C.; Lambla, M.; Spiess, H. W. *Macromolecules* **1996**, *29*, 5972.
(58) (a) Pérez, E.; Lang, J. *Langmuir* **1996**, *12*, 3180. (b) Marion, P.; Beinert, G.; Juhué, D.; Lang, J. *Macromolecules* **1997**, *30*, 123.
(59) Feng, J.; Odrobina, E.; Winnik, M. A. *Macromolecules* **1998**, *31*, 5290.

MA990561E